Ultrasonics - Sonochemistry 66 (2020) 105087

Contents lists available at ScienceDirect

Ultrasonics - Sonochemistry

journal homepage: www.elsevier.com/locate/ultson

The use of non-cavitating coupling fluids for intensifying sonoelectrochemical processes

Md Hujjatul Islam[a], Bouzid Naidji[b], Loic Hallez[b], Abdeslam Et Taouil[b], Jean-Yves Hihn[b,*], Odne S. Burheim[a], Bruno G. Pollet[a,*]

[a] Hydrogen Energy and Sonochemistry Research Group, Department of Energy and Process Engineering, Norwegian University of Science and Technology (NTNU), NO-7491 Trondheim, Norway
[b] Institut UTINAM UMR 6213 CNRS, Université de Bourgogne Franche Comte, 16 route de Gray F25030, Besançon Cedex, France

ARTICLE INFO

Keywords:
Sonoelectrochemistry
Double cell sonoreactor
Coupling fluid
Mass transfer
Asymmetric cavitation

ABSTRACT

For the first time, we have investigated the beneficial effects of non-cavitating coupling fluids and their moderate overpressures in enhancing mass-transfer and acoustic energy transfer in a double cell micro-sonoreactor. Silicon and engine oils of different viscosities were used as non-cavitating coupling fluids. A formulated monoethylene glycol (FMG), which is a regular cooling fluid, was also used as reference. It was found that silicon oil yielded a maximum acoustic energy transfer (3.05 W/cm^2) from the double jacketed cell to the inner cell volume, at 1 bar of coupling fluid overpressure which was 2.5 times higher than the regular FMG cooling fluid. It was also found that the low viscosity engine oil had a higher acoustic energy value than that of the high viscosity engine oil. In addition, linear sweep voltammograms (LSV) were recorded for the quasi-reversible $Fe^{2+/}Fe^{3+}$ redox couple (equimolar, 5×10^{-3} M) on a Pt electrode in order to determine the mass-transport limited current density (j_{lim}) and the dimensionless Sherwood number (*Sh*). From the LSV data, a statistical analysis was performed in order to determine the contribution of acoustic cavitation in the current density variation $|\Delta j|_{average}$. It was found that silicon oil at 1 bar exhibited a maximum current density variation, $|\Delta j|_{average}$ of ~2 mA/cm^2 whereas in the absence of overpressure, the high viscosity engine oil led to a maximum $|\Delta j|_{average}$ which decreased gradually with increasing coupling fluid overpressure. High viscosity engine oil gave a maximum *Sh* number even without any overpressure which decreased gradually with increasing overpressure. The *Sh* number for silicon oil increased with increasing overpressure and reached a maximum at 1 bar of overpressure. For any sonoelectrochemical processes, if the aim is to achieve high mass-transfer and acoustic energy transfer, then silicon oil at 1 bar of overpressure is a suitable candidate to be used as a coupling fluid.

1. Introduction

Sonoelectrochemistry is an interdisciplinary field of research where ultrasound is combined with electrochemistry, allowing the intensification of several processes. The evidence of coupling ultrasound with an electrochemical process dates back to the 1930́s when Moriguchi et al. [1] showed that water electrolysis using a platinum electrode could be enhanced by ultrasound. From the beginning of the 1990́s, there has been renewed interest in sonoelectrochemistry in the area of electrosynthesis [2–4], electroanalysis [5,6], nanomaterial synthesis [7] and electroplating [8–10]. Coupling ultrasound with an electrochemical system leads to some particular advantages such as: disruption and thinning of the *Nernst* diffusion layer and continuous cleaning and activation of the electrode surface [4,11,12].

Based on the *Nernst* diffusion equation (Eq. (1)), the limiting current density (j_{lim}) increases with decreasing the diffusion layer thickness (δ).

$$j_{lim} = nFAD_oC * /\delta \quad (1)$$

where j_{lim} is the limiting current, n is the number of electrons transferred during the electrochemical process, F is the Faraday constant, A is the electrode area, D_o is the diffusion coefficient of the electroactive species, C^* is the bulk concentration of the electroactive species and δ is the diffusion layer thickness.

In the presence of ultrasound, the diffusion layer thickness can be reduced to < 1 μm. In addition, Coury et al. [13] demonstrated that sonication leads to a substantial increase in limiting current (I_{lim}) along with the electrode surface activation by eliminating surface oxides due to mechanical stirring. Bubble collapse occurs both symmetrical and

* Corresponding authors.
E-mail addresses: jean-yves.hihn@univ-fcomte.fr (J.-Y. Hihn), bruno.g.pollet@ntnu.no (B.G. Pollet).

https://doi.org/10.1016/j.ultsonch.2020.105087
Received 9 February 2020; Received in revised form 16 March 2020; Accepted 22 March 2020
Available online 23 March 2020
1350-4177/

asymmetrical in an electrolytic system. The symmetrical collapse at the electrolyte media (homogeneous system) promotes mass transfer and the asymmetrical collapse at the electrode surface (heterogenous system) results in electrode cleaning and activation [14].

Ultrasound affects not only the homogenous system that takes place in the bulk solution but also the heterogenous system involving the electrode surface and the electroactive species. The first possibility to act on the heterogeneous kinetic step is the continuous removal of a deposit originating from a competing reaction [15]. The second step is to modify the electrochemical system by hydroxyl radical (OH·) generation induced by sonolysis. A new reaction mechanism may arise in the homogenous system due to extreme conditions caused by the collapse of cavitation bubbles [16].

However, in order to harness these remarkable benefits of power ultrasound, an efficient and suitable sonoelectrochemical cell is required. Researchers around the world have tried several experimental configurations for sonoelectrochemical research. Several sonoelectrochemical cell configurations have been proposed. One concept is the direct immersion of the ultrasonic probe into the electrochemical cell i.e. by facing the ultrasonic probe to the working electrode (WE) at a known distance ($d_{US\text{-}WE}$) – "face-on" geometry. The ultrasonic probe is placed close to the working electrode surface allowing fast cleaning and efficient electrode activation. In addition, the transmitted ultrasonic intensity (ψ) and the distance between the electrode and the sonotrode tip ($d_{US\text{-}WE}$) can be controlled. However, this arrangement has some limitations such as, for example, contamination of the electrolyte due to erosion of the sonotrode tip and controlling the electrolyte temperature due to heating induced by ultrasonication. Another arrangement proposed by Reisse et al. [17] is to use the ultrasonic horn as the working electrode. This type of arrangement is "ideal" for sonoelectrochemical synthesis of nanomaterials where pulse electrolysis is used for the deposition of the nanomaterials into the sonoelectrode and pulse sonication is used for subsequent removal of the nanomaterials from the sonoelectrode [7].

One possible way to avoid electrolyte solution contamination and over-heating is to use a double-jacketed cell. A few double-jacketed cell configurations have been used in the field and some examples are illustrated in Fig. 1. The most basic setup is the immersion of an electrochemical cell into an ultrasonic bath (Fig. 1(a)). This type of setup leads to very poor transfer of acoustic energy from the ultrasonic bath to the electrochemical cell together with low cavitation activity. Hihn, Pollet et al. [18] presented a cell with a slant bottom (Fig. 1(b)). However, it was found that the transfer of acoustic energy for this configuration was not satisfactory. Therefore, a double jacketed cell using coupling fluid was designed (Fig. 2) for the first time by Klíma and Bernard [19]. In this configuration, the ultrasonic probe was placed outside the electrochemical cell. This configuration prevents the electrolyte contamination and ensures perfect electrical insulation from the ultrasonic transducer. The cooling fluid used in this arrangement also works as a coupling medium that allows efficient propagation of the ultrasonic energy from the transducer tip into the reactor solution. An overpressure of 4–5 atm was applied in the coupling medium for lowering the transient cavitation activity outside the cell. The acoustic intensity of 2 W/cm^2 was obtained at 20 kHz with an electrical output of 40 W/cm^2. Inspired by Klíma and Bernards work, Costa et al. [14] improved their design and obtained an acoustic intensity of > 0.60 W/cm^2 at 1.5 bar overpressure only by using a 20 kHz transducer with an electrical output of ~10 W/cm^2. Costa et al. [14] also studied the effect of overpressure on the heterogenous mass-transfer where they found that the Sherwood number (*Sh*) increased with increasing overpressure and increasing ultrasonic intensity (ψ).

However, the main problem in these types of configurations is the loss of maximum amount of ultrasonic energy into the coupling fluid due to cavitation and thus very poor transfer of ultrasonic energy into the electrochemical cell. In this case, the sonochemical activity inside the electrochemical cell is also negligible due to the lack of transient cavitation. Acoustic cavitation is the formation of cavitation bubble in the liquid during the propagation of intense ultrasonic wave i.e. a wave of pressure oscillation. In order to generate cavitation bubble, the local liquid pressure needs to be decreased to a pressure lower than the atmospheric pressure. During the rarefaction phase, the liquid experiences an instantaneous lower pressure than the atmospheric pressure causing tiny gas bubbles to form. In addition, in order to generate cavitation bubble, it is also necessary to increase the pressure-amplitude of rarefaction. The minimum acoustic amplitude required for cavitation bubble to form is called the "cavitation threshold". This threshold is often different from the bubble nucleation to occur since its strongly depends upon the degree of gas saturation in the liquid. The threshold pressure amplitude for cavitation increases as ultrasonic frequency increases; for example, the threshold pressures at different frequencies

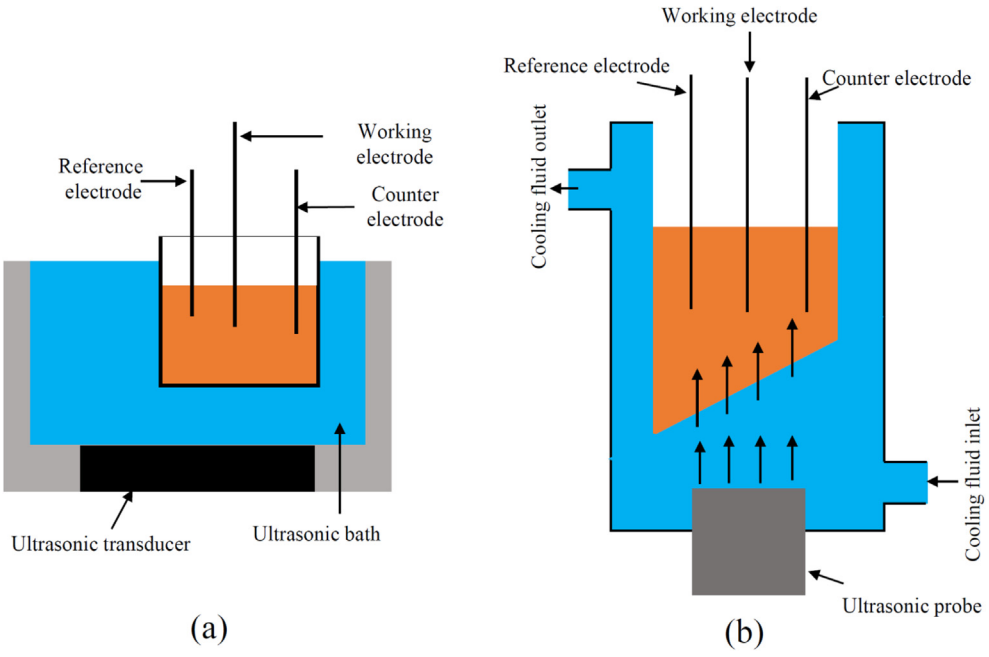

Fig. 1. Schematic diagram of the different double cell sonoelectrochemical configurations.

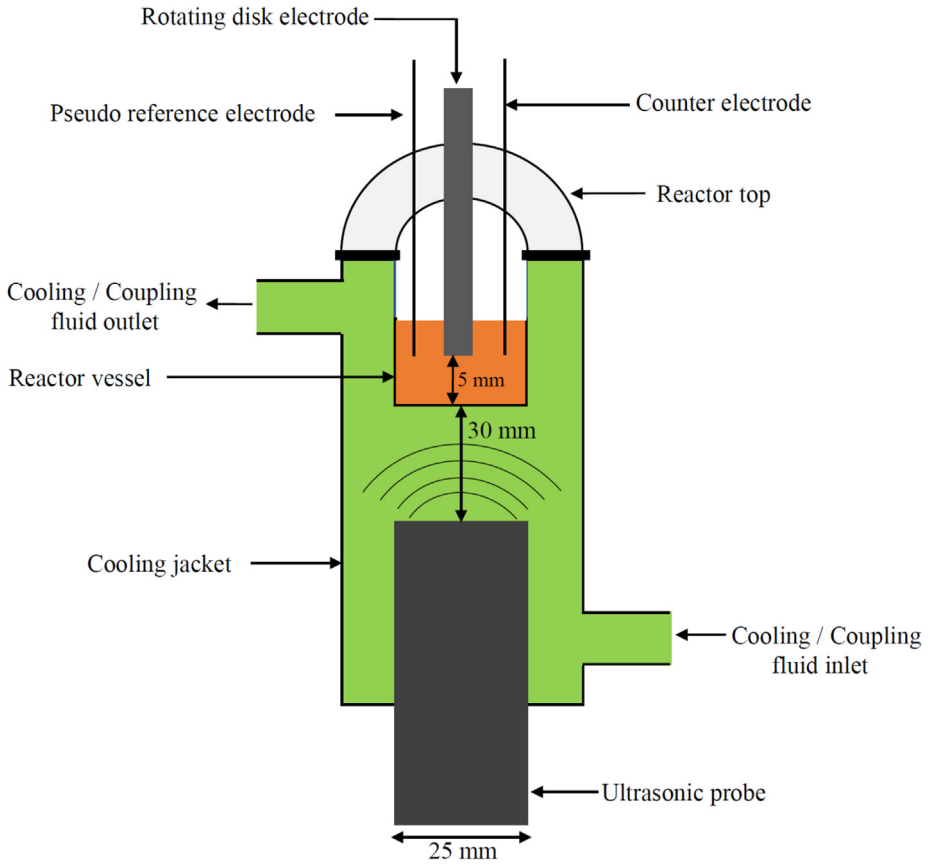

Fig. 2. Schematic diagram of the double cell micro-sonoreactor equipped with three electrode assembly (Besançon cell).

are 1.2 bar, 1.6 bar, 3 bar and 5.8 bar at 20 kHz, 140 kHz, 1 MHz and 5 MHz, respectively in pure water saturated with gas [20,21].

It is therefore challenging to transmit the ultrasonic energy from the cooling jacket into the reactor in a double cell micro-sonoreactor (Fig. 2, Besançon cell), since an amount of energy is dissipated into the cooling/coupling media. This useful energy is lost due to cavitation occurring in the coupling fluid [22]. If the cavitation activity is suppressed in the coupling fluid, then the travelling of the acoustic wave creates cavitation inside the electrochemical cell where there are favorable conditions for transient cavitation. There are several ways to suppress cavitation activity in a liquid. One is to increase the pressure of the coupling fluid higher than the cavitation threshold pressure. In this strategy, the ultrasonic wave travels through a high-pressure zone (the coupling medium) into an atmospheric pressure zone (the reactor volume). The cavitation activity is dampened in the high-pressure zone during the propagation of the ultrasonic wave and cavitation occurs in the atmospheric pressure zone. Another strategy is to use a degassed fluid where bubble nucleation is hindered due to the lack of dissolved gases.

For the first time, near non-cavitating fluids (high viscosity Newtonian and non-Newtonian fluids) were used as coupling media. Here, near non-cavitating fluids mean the fluids that marginally cavitate at atmospheric pressure and do not cavitate under modest overpressure (generally below or equal to acoustic threshold pressure). In this study, we present the role of near non-cavitating coupling fluids under overpressure conditions (0.5 and 1 bar) for the improvement of the acoustic energy transfer and heterogenous mass-transfer in a double-jacketed sonoelectrochemical cell (Fig. 2).

2. Methods and materials

2.1. Reactor design and experimental setup

Sonoelectrochemical experiments were carried out in a double wall reactor equipped with a Sinaptec transducer (NexTgen Lab750) operating at 20 kHz (Fig. 2). The working volume of the inner cell (micro-sonoreactor) was 7 ml. A Process Flow Diagram (PFD) for the coupling fluid circulation system is illustrated in Fig. 3. In the PFD diagram illustrated in Fig. 2, the valve 1 and valve 2 were placed at the inlet and outlet of the cooling jacket allowing to close the coupling fluid circulation completely during acoustic power measurement. A pressure gauge was placed before valve 2 to measure the overpressures present in the cooling jacket. The different coupling fluids were placed in an open vessel. The fluids were pumped through a heat-exchanger for efficient cooling of the coupling fluid, which were heated due to ultrasonication. Valve 3 was used to regulate the pressure inside the cooling jacket and to by-pass the coupling fluid when valve 1 was closed. The distance between the top of the sonotrode and the inner cell bottom was 30 mm (Fig. 3), and the disc electrode (DE) was placed 5 mm above the bottom of the reactor. For the electrochemical mass transfer measurement and acoustic power measurement, overpressures of 0.5 and 1 bar in the coupling fluid were applied using an external pump.

Three (3) coupling fluids were studied, namely: (i) a water like Formulated Monoethylene Glycol (FMEG − 30% monoethylene glycol + 70% water) used as reference, (ii) a silicon oil (polydimethyl siloxane) and. (iii) an engine oil. Table 1 shows the physicochemical properties of the coupling fluids used in this study.

2.2. Mass-transfer measurements

Mass-transfer measurements were performed using a three-

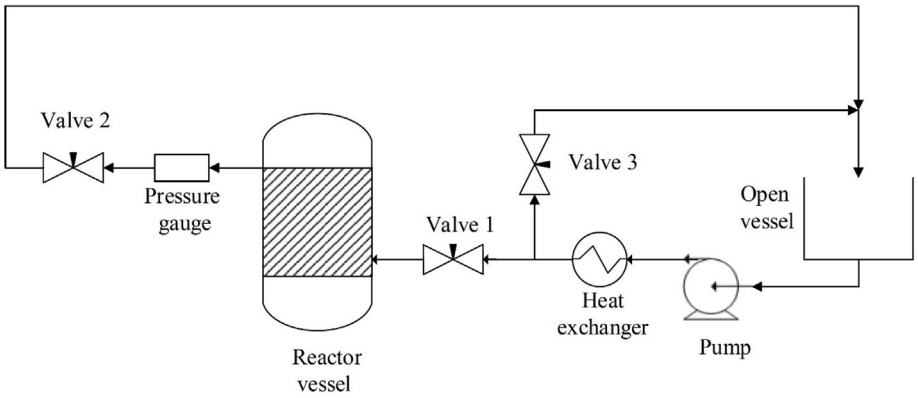

Fig. 3. The Process Flow Diagram (PFD) of the coupling fluid circulation system. Here, the reactor vessel is the double cell micro-sonoreactor as shown in Fig. 2.

electrode assembly as illustrated in Fig. 2. The working electrode (WE) was a platinum disc electrode (DE, ∅ = ~3 mm). The disc electrode was not rotating during the recording of the current–potential polarization curves. The WE was placed in a 'face-on' geometry, where the transducer tip and the electrode were facing each other at a distance of ~35 mm. Platinum wires (Approximately 15 mm immersion length with 1 mm of diameter) of high purity were used as quasi-reference (REF) and counter (CE) electrodes. An Autolab PGSTAT-302 N potentiostat and an Autolab Disc Electrode (DE) from Metrohm was used for all electrochemical measurements. Before each experiment, the DE tip was polished using a mechanical polishing machine GRINDPOL1 to mirror finish using diamond suspension of decreasing size down to 0.25 µm. The platinum wires used as *pseudo* REF and CE were immersed in 25% H_2SO_4 solution for 10 min and then rinsed with distilled water. Since ultrasonication is able to alter the properties of the electrolyte, a new solution was used for consecutive experiments. An equimolar quasi-reversible redox couple of 0.005 M $Fe^{2+/}Fe^{3+}$ was used. $K_4Fe(CN)_6{\cdot}3H_2O$ (CAS: 14459-95-1) and $K_3Fe(CN)_6$ (CAS: 13746-66-2), were purchased from Alfa Aesar and used as Fe^{2+} and Fe^{3+} respectively in 0.2 M Na_2SO_4 (CAS: 7757-82-6, purchased from Sigma-Aldrich). Cyclic voltammograms (CV) and linear cyclic voltammograms (LSV) were recorded under steady-state conditions at a scan rate of 2 mV/s. Before recording LSVs, the CVs were recorded each time, showing typical sigmoidal shapes (not presented here) to ensure that the electrochemical system (both electrodes and the electrolytes) functioned well.

2.3. Acoustic power measurements

Acoustic power measurements were carried out by ultrasonicating 5 ml ultrapure water for 1 min. The temperature increase, due to the conversion of mechanical energy into heat, was recorded every second by using a National Instruments thermocouple controlled by a LabView software. For the acoustic power measurement in the absence of coupling fluid overpressure, the valve 1 and valve 2 were closed, and then the ultrapure water sonicated for 60 s. For sonication experiments involving an overpressure of the coupling fluid, at first the valve 2 was closed. Then the valve 1 was regulated by keeping the valve 3 open in such a way that the desired overpressure in the cooling jacket was obtained as soon as the valve 1 was fully closed. Then sonication was carried out for 1 min at the desired overpressure. During the sonication in the closed system of the coupling fluid, the pressure tended to rise from the desired pressure. In that case, the valve 2 was released slightly to decrease the increased pressure from the required pressure. Finally, the calorimetric power was calculated using the method presented by Mason et al. [23] and Contamine et al. [24]. In our conditions, the slopes of the time-dependent temperature change showed linearity as expected. The calorimetric power measurement results were then presented as acoustic intensity, ψ (in W/cm^2) where the acoustic power (P_T in W) was divided by the area of the ultrasonic emitting device ($A_{US\ tip}$ in cm^2).

3. Results and discussion

3.1. Ultrasonic energy transmission into the double cell

Fig. 4 shows the experimental set-up using the silicon oil in the outer cell, acting as a cooling fluid as well as a coupling medium. The inner cell shows the 0.005 M $Fe^{2+/}Fe^{3+}$ redox couple in 0.2 M Na_2SO_4 and ultrapure water. It can be observed that, at atmospheric pressure (Fig. 4(a)), cavitation is intense in the silicon oil, particularly at the ultrasonic horn surface. A "bubble cone" is clearly visible [25] indicating that the acoustic activity can freely occur in this fairly viscous fluid (~5 times more than water). This observation also suggests a loss of energy into the fluid, as the energy used for cavitation will never reach the inner cell and therefore will not greatly affect any chemical or electrochemical processes. By increasing the overpressure to 0.5 bar in the outer cell (Fig. 4(b)), it can be seen that the number of bubbles decreases in the coupling fluid, and the global cavitation distribution follows another pattern, well organised in streams of bubbles. Increasing further the overpressure to 1 bar (Fig. 4(c)), a decrease in acoustic activity becomes evident, and the cavitation is dampened at the vicinity of the ultrasonic horn. Therefore, it is clear that at 1 bar of overpressure, the silicon oil acts like a non-cavitating fluid ensuring a maximum amount of energy transfer from the coupling medium into the inner cell volume. Indeed, a visual observation of the inner cell indicated an increase in solution mixing. Further experiments were carried out up to 1.5 bar of overpressure (not shown here) whereby it was found that cavitation was completely quenched, but the ultrasonic generator, influenced by impedance modification, was not operating steadily. In this study, we have limited the overpressure up to 1 bar.

Table 1
Physico-chemical properties of coupling fluids.

Fluid name	Density (kg/m^3)	Viscosity (Pa.s)	Supplier
Formulated Monoethylene Glycol (FMEG) (30% Monoethylene glycol + 70% water)	1000	0.001	Commercial engine coolant
Silicon oil (Polydimethyl siloxane)	960	0.005	Purchased from VWR (Article no. 24610.363)
Engine oil (15 W-40)	870	0.03	Commercial name: Total ACTIVA

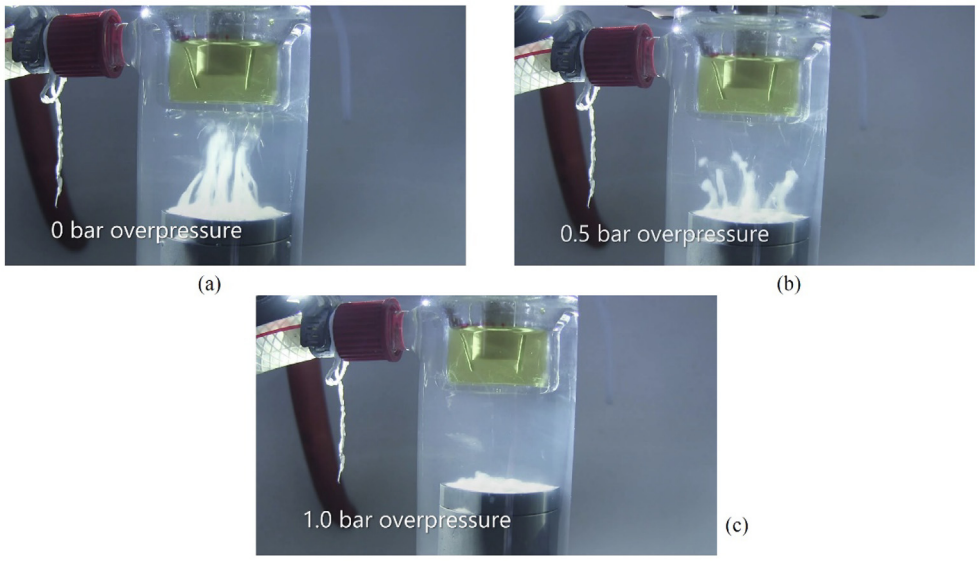

Fig. 4. Effect of various overpressures on the cavitation activity of silicon oil. Here silicon oil works both as a cooling and a coupling media for ultrasonic wave propagation (a) 0 bar overpressure (atmospheric) in the coupling fluid, (b) 0.5 bar overpressure and (c) 1.0 bar overpressure [22].

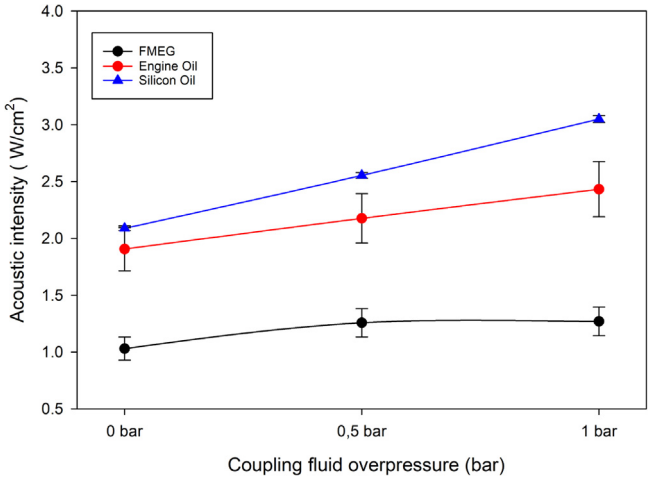

Fig. 5. Effect of different coupling fluid overpressures on the ultrasonic energy transfer from the coupling media to the inner cell at 80% of acoustic amplitude.

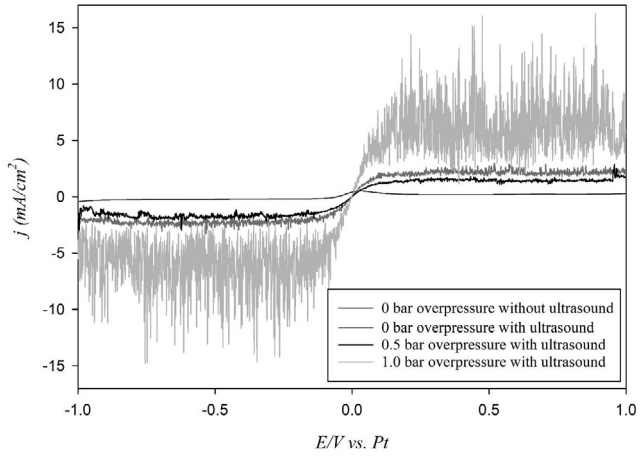

Fig. 6. Linear sweep voltammograms (LSV) of Fe^{3+}/Fe^{2+} quasi-reversible couple (equimolar, 0.005 M) in 0.2 Na_2SO_4 on Pt under steady-state conditions at different silicon oil overpressures.

Fig. 5 shows the effect of the coupling fluid overpressures on the transmitted acoustic power (P_T) from the coupling media to the reactor (measured in the inner cell) for the three coupling fluids (for these specific measurements, the fluid was not circulating). It may be observed that for all coupling media, the transmitted acoustic power increases while increasing the overpressure, with P_T values being much higher with both oils compared to the regular cooling fluid (FMEG). This observation was also confirmed when plotting the data as a function of the acoustic amplitude in the range 50% – 80% at 1 bar (not shown here). For silicon oil, corresponding to an increase in the kinematic viscosity from 10^{-3} m^2/s to 5.10^{-3} m^2/s, the transmitted acoustic power is clearly higher. However, for the high viscosity engine oil (30.10^{-3} m^2/s), the transmitted power is lower. Several phenomena may explain this behaviour. From one hand, using higher viscosity fluids, the ultrasonic wave reflection is higher, so that for a given ultrasonic horn amplitude, a part of the ultrasonic energy reflected by the coupling media is higher. From another hand, the viscosity is far from being the only parameter driving the ultrasonic transmission, as commercial oils have complex rheological behaviour. The ultrasound attenuation is equally influenced by several other fluid properties, such as sound velocity as described in the literature [26]. Even if the available data concern mostly higher ultrasonic frequencies [27], it can be said that the speed of sound do not vary proportionally with fluid viscosity. Thus, additional calorimetric measurements were performed on the various fluids (in a beaker and at atmospheric conditions) to determine the transmitted ultrasonic power for a given ultrasonic amplitude (50%). Under similar conditions, the temperature rates were found to be as follows: FMEG, 4.35 °C/min – high viscosity engine oil, 11 °C/min and silicon oil, 13.23 °C/min. These temperature rates are quite high suggesting that the coupling media are subjected to an increase in temperature under the transmitted ultrasonic power measurement conditions. Thus, heat transmission from coupling fluid to the inner cell is permitted, in turn affecting the transmitted ultrasonic power measurements. Finally, and more importantly, the main drawback for using coupling media, is the temperature control in the inner cell, which is very challenging. Proper design parameters, including high coupling/contact area between the coupling fluid and the reactor as well as high circulation fluid flowrates are required for all mass-transfer measurements.

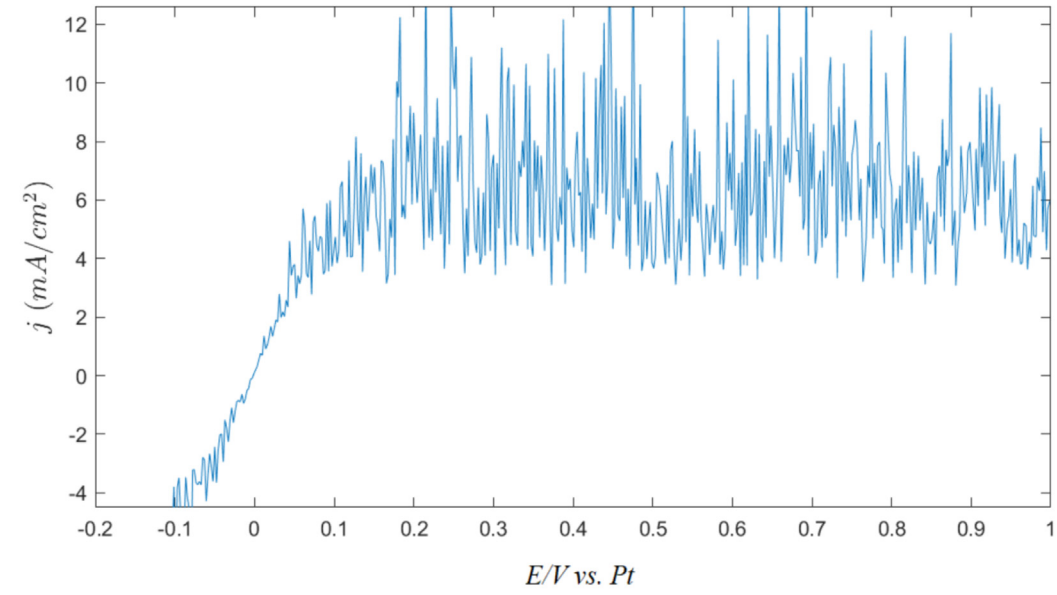

(a)

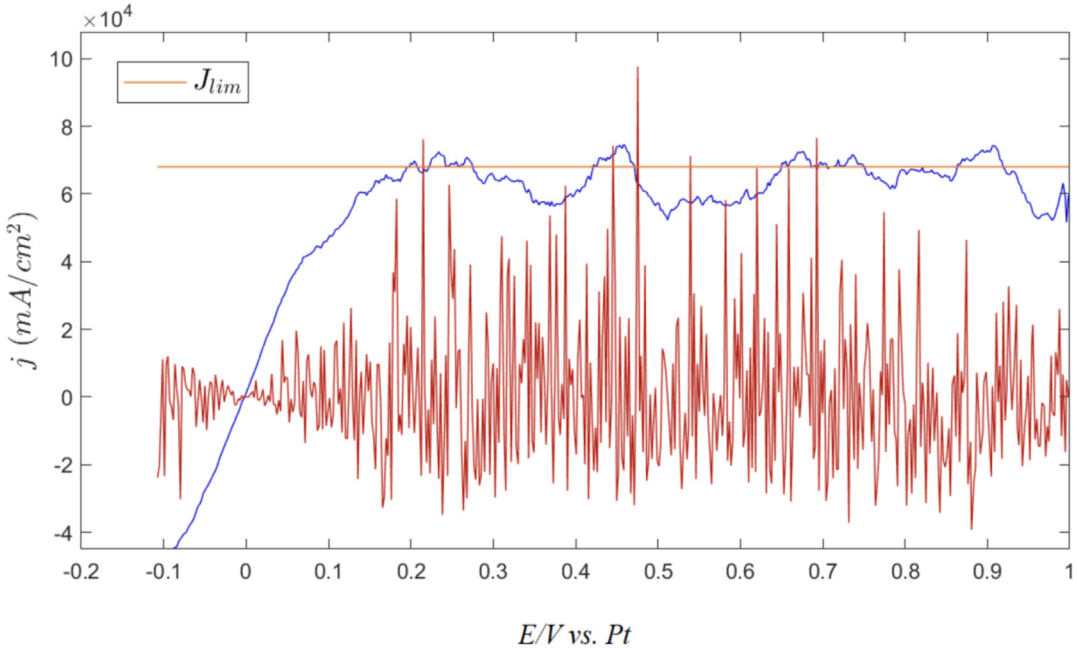

(b)

Fig. 7. Example of data processing and discretization of contributions from cavitation. (a) $j = f(E)$ is the raw current measurement for 0.005 M Fe^{3+}/Fe^{2+} solution where silicon oil was used as coupling fluid at 1 bar overpressure and 50% acoustic amplitude. (b). The smoothing of the raw data is plotted in blue and the red line shows the subtraction of the smoothing values from the raw data. (For interpretation of the references to colour in this figure legend, the reader is referred to the web version of this article.)

3.2. Mass-transfer enhancement

In order to study the effect of different coupling fluids and their overpressures, a series of linear sweep voltammograms (LSV) of equimolar Fe^{2+}/Fe^{3+} quasi-reversible couple were recorded in the potential range [+1.0 – −1.0 V *vs.* Pt]. For all electrochemical experiments, the coupling fluids were circulating and cooled, in order to keep an average electroanalyte temperature of ~20 °C in the inner cell. The LSVs at different overpressures for silicon oil as coupling fluid are shown in Fig. 6. The figure shows typical "S" shaped voltammograms at high potentials (both positive and negative) for a quasi-reversible redox couple indicative of mass transfer limitations. In addition, highly disturbed signals with large fluctuations are observed, mainly caused by the vigorous movement of the electroanalyte due to acoustic streaming, turbulent flow and implosion of cavitation bubbles in the form of microjets on the electrode surface. The signal intensities in the plateau regions are fairly moderate at 0 and 0.5 bar of overpressure. However, at 1 bar of overpressure, the signal intensities in the two plateau regions are intense suggesting very high transient cavitation activity in the inner cell. This finding is in good agreement with the visual observation in Fig. 4(c), where at 1 bar of overpressure, almost no cavitation in the coupling media was observed and intense transient cavitation activity occurred. Under ultrasonic irradiation, the mass-transfer limited currents include a steady-state and a time dependent component. The time

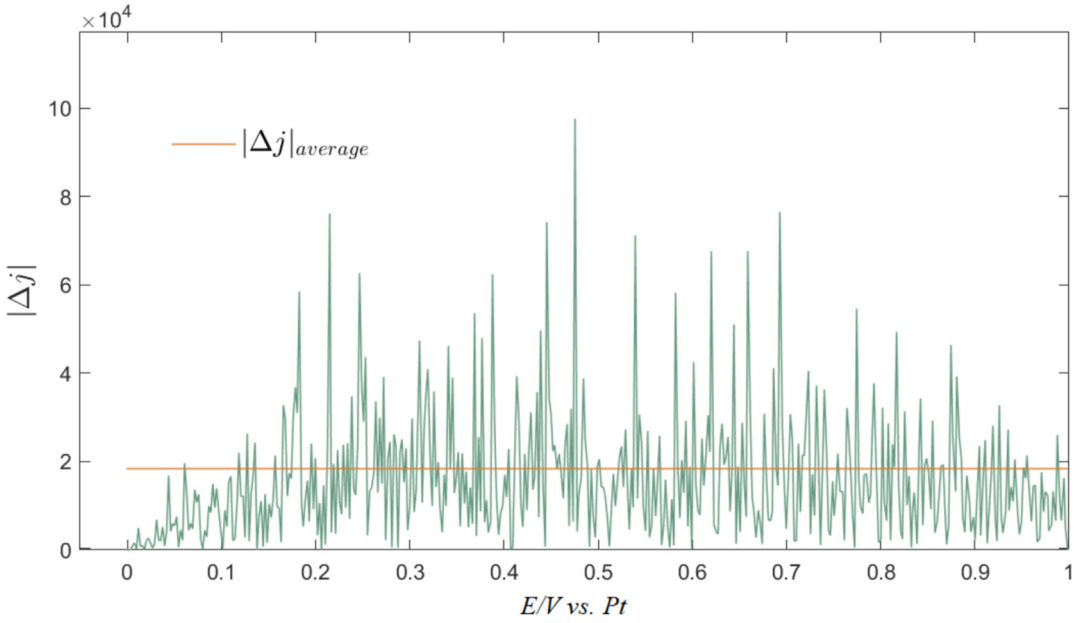

Fig. 8. Example of raw data processing for the determination of $|\Delta j|_{average}$.

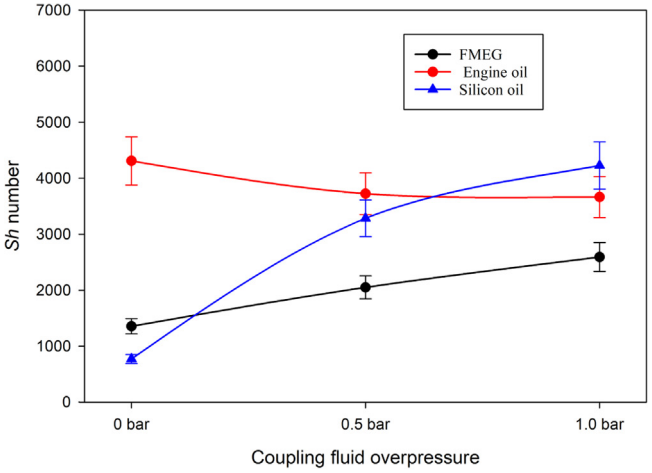

(a)

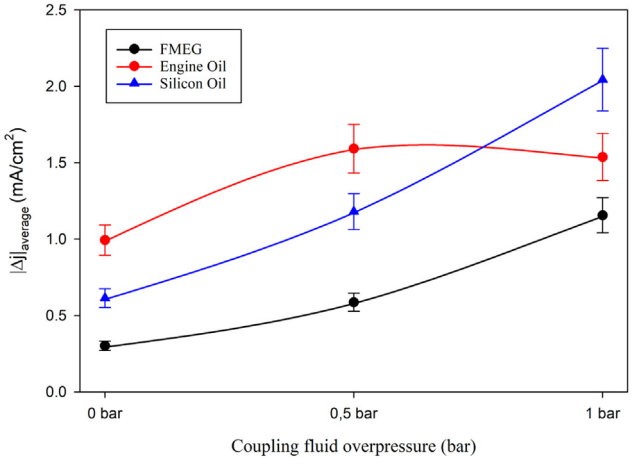

(b)

Fig. 9. . (a) *Sh* number as a function of different coupling fluid overpressures at 70% acoustic amplitude (b). Evolution of the average current density variation as a function of coupling fluid overpressure for different coupling fluids.

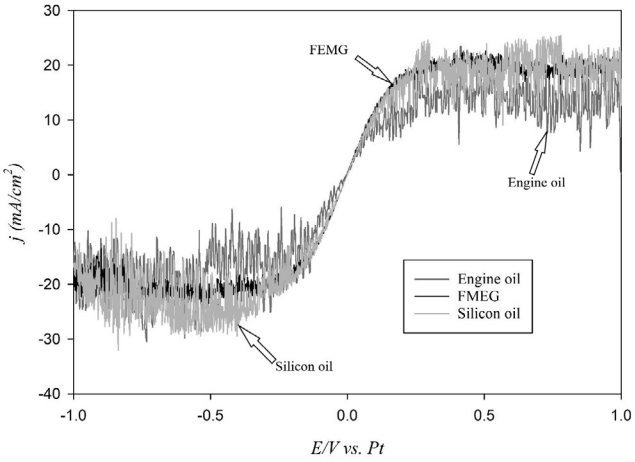

Fig. 10. Current-potential polarization curves of the Fe^{3+}/Fe^{2+} reversible couple under steady-state conditions at 1 bar overpressure and 70% of acoustic amplitude.

dependent component is the oscillation of the current signals around the average current plateau, which is mainly attributed to cavitation activities. In this case, the acoustic cavitation bubbles either oscillate at the electrode surface or collapse violently in the form of microjets at the surface causing a fluctuation in current pulses. The global agitation level in an electrochemical cell under ultrasonic conditions is usually a combination of acoustic streaming, turbulent flow and asymmetric bubble collapse (micro-jets) at the electrode surface.

In order to determine the contributions in the observed increased currents, a statistical data processing was performed on the LSV curves using the "smooth function" in *Matlab* calculating a moving average on 30 data points before and after the considered data. The time dependent component related to cavitational events and the average current density values (j_{lim}) corresponding to the global agitation in the inner cell were extracted through such a data processing strategy (Fig. 7) [28]. Sherwood (*Sh*) numbers were calculated from the limiting current density (j_{lim}), allowing to regroup all contributions (i.e. convection as well as asymmetric cavitation) to the global agitation at the electrode surface. This *Sh* number allows to characterize the mass-transport efficiency, i.e. the dimensionless number which does not depend upon the

electrochemical parameters such as the electrode geometry, the nature of the solvent and the electroactive species. From the j_{lim} values, Eq. (2) was used to calculate the Sherwood number (*Sh*).

$$Sh = \frac{J_{\lim} r_p}{nFCD} \quad (2)$$

Here, r_p the radius of the DE tip (m), D the diffusion coefficient of the electroactive specie (m^2/s), j_{lim} is the mass-transfer limited current density (A/m^2), n is the number of transferred electrons, F the Faraday number (96,500C/mol) and C is the concentration of the electroactive species (mol/m^3) [14]. In order to understand the cavitational activity and to quantify the contributions of the elevated mass-transport, a complementary data analysis was performed to the raw LSV data. The resulting data from the statistical processing were subtracted from the raw data and the signal (noise) used to separate the time-dependent component. This time dependent component is usually composed of the current oscillation around the limiting current average value corresponding to the cavitational activity. The determination of the absolute average values in these highly oscillated signals $|\Delta j|_{average}$ (Fig. 8) is an excellent indicator of the cavitational activity inside the inner cell.

The Sherwood numbers and $|\Delta j|_{average}$ at different overpressures and various coupling fluids are shown in Fig. 9(a) and Fig. 9(b) respectively. For FMEG and silicon oil, both Sherwood numbers and $|\Delta j|_{average}$ increase gradually while increasing the overpressure in the cooling fluid, indicating that the global agitation increases as well as the contribution from asymmetric cavitation. For silicon oil, the Sherwood number in the absence of overpressure is even lesser than that of the FMEG. Comparing with literature, the Sherwood number at 1 bar of overpressure for FMEG as coupling fluid is ca. 900 at maximum acoustic amplitude [14]. But, at similar overpressure and acoustic amplitude, the silicon oil leads to a 4.5 times higher Sherwood number than FMEG, reaching a maximum of 4227 at 1 bar (Fig. 9(a)). In these conditions, the high values of $|\Delta j|_{average}$ indicate that the dominant contributor in the global agitation is the presence of micro-jets induced by cavitation.

However, the behaviour of the high viscosity engine oil is completely different. In the absence of overpressure, the Sherwood number is the highest for all conditions (4424), even over Sherwood numbers recorded for silicon oil at 1 bar overpressure, but with a weaker contribution from asymmetric cavitation. The acoustic streaming and turbulent flow are the dominant phenomena in the inner cell when high viscosity engine oil is used as coupling fluid without overpressure. Increasing the overpressure yields a continuous decrease in the Sherwood numbers (Fig. 9(a)) and a decrease in $|\Delta j|_{average}$ (Fig. 9(b)). One possible explanation resides in the reduction in the coupling fluid viscosity due to cavitation. Time and Rabenjafimanantsoa [29] have highlighted that cavitation is responsible for the reduction in viscosity for highly viscous fluids due to chemo-mechanical degradation. When more and more ultrasonic pulses are generated, pockets of fluid with lower viscosity are formed in between the high viscosity areas, affecting the ultrasonic wave transmission [29]. Moreover, at 1 bar of overpressure which is close to the cavitation threshold, the high viscosity engine oil may act more like a solid than a liquid, contributing to the vibration of the whole reactor, including the inner cell. This may impact the ultrasonic transmission and particularly the cavitational activity within the inner cell, yielding lower $|\Delta j|_{average}$ at 1 bar of overpressure. On the contrary, Time and Rabenjafimanantsoa [29] does not report formation of low viscosity pockets in mineral oil, due to its higher thermal stability. This is also true for the Sherwood number plots (Fig. 9(a)).

Finally, LSVs for different coupling fluids at 1 bar and 70% acoustic pressure (Fig. 10) confirm that viscous fluids such as high viscosity engine oil and silicon oil exhibited high oscillated signals in the mass transport limited regions i.e. higher asymmetric cavitational events than those observed for FMEG; although silicon oil was found to be the only fluid exhibiting both a good global agitation and a good cavitational activity. From our studies, the best conditions to perform sonoelectrochemical experiments are those using silicon oil as coupling fluid operating at 1 bar in a double-jacketed sono-reactor.

4. Conclusions

The use of non-cavitating coupling fluids with marginal overpressures in a double-jacketed cell sono-reactor for sonoelectrochemistry is a promising approach for improving mass transfer and to obtain fairly high transfer of acoustic energy from the coupling media to the reactor inner cell. In our conditions, it was found that the silicon oil at 1 bar of overpressure and high viscosity engine oil in the absence of any overpressures ensured efficient mass and acoustic energy transfers. In addition, all the non-cavitating coupling fluids yielded higher acoustic intensity than conventional FMEG. The high viscosity engine oil also led to high Sherwood numbers in the absence of overpressure, and the silicon oil at 1 bar of overpressure provided the best results in both Sherwood number and $|\Delta j|_{average}$ values. These non-cavitating coupling fluids may be advised for sonoelectrochemical experiments in which higher acoustic intensity effects are required.

Acknowledgements

Md.H. Islam and B.G. Pollet would like to thank the ENERSENSE research initiative at NTNU for the financial support to perform the experimental activities at the UTINAM laboratories, the University of Franche-Comté (UFC), Besançon, France. They also thank the UTINAM research team and the laboratory support staff for their valuable support in carrying out the experiments.

References

[1] N. Moriguchi, The influence of supersonic waves on chemical phenomena. III The influence on the concentration polarisation, Nippon KAGAKU KAISHI 55 (8) (1934) 749–750.
[2] B. Pollet, J.P. Lorimer, S.S. Phull, J.Y. Hihn, Sonoelectrochemical recovery of silver from photographic processing solutions, Ultrason. Sonochem. 7 (2) (2000) 69–76.
[3] N. Neha, M.H. Islam, S. Baranton, C. Coutanceau, B.G. Pollet, Assessment of the beneficial combination of electrochemical and ultrasonic activation of compounds originating from biomass, Ultrason. Sonochem. (Dec. 2019) 104934.
[4] M.H. Islam, O.S. Burheim, B.G. Pollet, Sonochemical and sonoelectrochemical production of hydrogen, Ultrason. Sonochem. 51 (Mar. 2019) 533–555.
[5] J.-Y. Hihn, M.-L. Doche, A. Mandroyan, L. Hallez, B.G. Pollet, Respective contribution of cavitation and convective flow to local stirring in sonoreactors, Ultrason. Sonochem. 18 (4) (Jul. 2011) 881–887.
[6] E.L. Cooper, L.A. Coury, Mass transport in sonovoltammetry with evidence of hydrodynamic modulation from ultrasound, J. Electrochem. Soc. 145 (6) (1998) 1994–1999.
[7] M. Hujjatul Islam, M.T.Y. Paul, O.S. Burheim, B.G. Pollet, Recent developments in the sonoelectrochemical synthesis of nanomaterials, Ultrason. Sonochem. 59 (Dec. 2019) 104711.
[8] A. Chiba, W.C. Wu, Ultrasonic agitation effects on the electrodeposition of copper from a cupric-EDTA bath, Plat. Surf. Finish. 79 (12) (1992) 62–66.
[9] Aymeric Nevers, Loïc Hallez, Francis Touyeras, Jean-Yves Hihn, Effect of ultrasound on silver electrodeposition: crystalline structure modification, Ultrason. Sonochem. 40 (2018) 60–71, https://doi.org/10.1016/j.ultsonch.2017.02.033.
[10] K. Kobayashi, A. Chiba, N. Minami, Effects of ultrasound on both electrolytic and electroless nickel depositions, Ultrasonics 38 (1–8) (Mar. 2000) 676–681.
[11] T.J. Mason, V.S. Bernal, An introduction to sonoelectrochemistry, Power Ultrasound in Electrochemistry, John Wiley & Sons, Ltd, 2012, pp. 21–44.
[12] B.G. Pollet, Does power ultrasound affect heterogeneous electron transfer kinetics? Ultrason. Sonochem. 52 (Apr. 2019) 6–12.
[13] N.A. Madigan, C.R.S. Hagan, H. Zhang, L.A. Coury, Effects of sonication on electrode surfaces and metal particles, Ultrason. Sonochem. 3 (3) (Nov. 1996) S239–S247.
[14] C. Costa, J.Y. Hihn, M. Rebetez, M.L. Doche, I. Bisel, P. Moisy, Transport-limited current and microsonoreactor characterization at 3 low frequencies in the presence of water, acetonitrile and imidazolium-based ionic liquids, Phys. Chem. Chem. Phys. 10 (2008) 2149–2158.
[15] B. Pollet, J.P. Lorimer, J.-Y. Hihn, F. Touyeras, T.J. Mason, D.J. Walton, Electrochemical study of silver thiosulphate reduction in the absence and presence of ultrasound, Ultrason. Sonochem. 12 (1–2) (Jan. 2005) 7–11.
[16] B.G. Pollet, Power Ultrasound in Electrochemistry: From Versatile Laboratory Tool to Engineering Solution, Wiley, 2012.
[17] J. Reisse, et al., Sonoelectrochemistry in aqueous electrolyte: a new type of sonoelectroreactor, Electrochim. Acta 39 (1) (Jan. 1994) 37–39.
[18] J.-Y. Hihn, et al., Double-structured ultrasonic high frequency reactor using an

optimised slant bottom, Ultrason. Sonochem. 7 (4) (Oct. 2000) 201–205.
[19] J. Klíma, C. Bernard, Sonoassisted electrooxidative polymerisation of salicylic acid: Role of acoustic streaming and microjetting, J. Electroanal. Chem. 462 (2) (1999) 181–186.
[20] K. Yasui, Acoustic cavitation and bubble dynamics. SpringerBriefs in Molecular Science: Ultrasound and Sonochemistry, 2018.
[21] K. Yasui, Dynamics of acoustic bubbles, in: Sonochemistry and the Acoustic Bubble, Elsevier, 2015, pp. 41–83.
[22] M.H. Islam, J.J. Lamb, K.M. Lien, O.S. Burheim, J.-Y. Hihn, B.G. Pollet, (Invited) novel fuel production based on sonochemistry and sonoelectrochemistry, ECS Trans. 92 (10) (2019) 1–16.
[23] T.J. Mason, Sonochemistry: The Uses of Ultrasound in Chemistry, Royal Society of Chemistry, Cambridge, 1990.
[24] R.F. Contamine, A.M. Wilhelm, J. Berlan, H. Delmas, Power measurement in sonochemistry, Ultrason. Sonochem. 2 (1) (Jan. 1995) S43–S47.
[25] A. Moussatov, C. Granger, B. Dubus, Ultrasonic cavitation in thin liquid layers, Ultrason. Sonochem. 12 (6) (Aug. 2005) 415–422.
[26] S. Yao, S. Mettu, S.Q.K. Law, M. Ashokkumar, G.J.O. Martin, The effect of high-intensity ultrasound on cell disruption and lipid extraction from high-solids viscous slurries of Nannochloropsis sp. biomass, Algal Res. 35 (Nov. 2018) 341–348.
[27] G.G. Stokes, On a difficulty in the theory of sound, Springer New York, New York, NY, 1998, pp. 71–81.
[28] B. Naidji, L. Hallez, A.E. Taouil, M. Rebetez, J.Y. Hihn, Influence of pressure on ultrasonic cavitation activity in room temperature ionic liquids: an electrochemical study, Ultrason. Sonochem. 54 (2019) 129–134.
[29] R.W. Time, A.H. Rabenjafimanantsoa, Cavitation bubble regimes in polymers and viscous fluids, Annu. Trans. Nord. Rheol. Soc. 19 (2011).